Inhibitory Role of Gas6 in Intestinal Tumorigenesis

Reiko Akitake-Kawano[1], Hiroshi Seno[1]*, Masato Nakatsuji[1], Yuto Kimura[1], Yuki Nakanishi[1], Takuto Yoshioka[1], Keitaro Kanda[1], Mayumi Kawada[1], Kenji Kawada[2], Yoshiharu Sakai[2], Tsutomu Chiba[1]

[1]Department of Gastroenterology and Hepatology, [2]Department of Surgery, Kyoto University Graduate School of Medicine, 54 Shogoin-Kawahara-cho, Sakyo-ku, Kyoto, Japan 606-8507.

***To whom correspondence should be addressed.** Tel: 81-75-751-4319**;** Fax: 81-75-751-4303**;** E-mail: seno@kuhp.kyoto-u.ac.jp

Short title:

Gas6 suppresses intestinal tumorigenesis

Keywords:

cancer, colon, innate immunity, colitis, *Apc*^{Min}

Disclosures:

All authors have no conflict of interests.

Abstract

Growth arrest-specific gene (Gas) 6 is a Gla domain-containing protein which shares 43% amino acid identity with protein S. Gas6 has been shown to enhance cancer cell proliferation *in vitro*. On the other hand, recent studies have demonstrated that Gas6 inhibits Toll-like receptor-mediated immune reactions. Immune reactions are known to affect intestinal tumorigenesis. In this study, we investigated how Gas6 contributes to tumorigenesis in the intestine. Administration of recombinant Gas6 weakly, but significantly, enhanced proliferation of intestinal cancer cells (SW480 and HT29), while it suppressed the inflammatory responses of LPS-stimulated monocytes (THP-1). Compared with *Gas6*$^{+/+}$ mice, *Gas6*$^{-/-}$ mice exhibited enhanced azoxymethane/dextran sulfate sodium (DSS)-induced tumorigenesis and had a shorter survival. *Gas6*$^{-/-}$ mice also exhibited more severe DSS-induced colitis. DSS-treated *Gas6*$^{-/-}$ mice showed attenuated Socs1/3 mRNA expression and enhanced NFκB activation in the colonic stroma, suggesting that the target of Gas6 is stromal cells. Bone marrow transplantation experiments indicated that both epithelial cells and bone marrow-derived cells are Gas6 sources. Furthermore, the number of intestinal tumors in *Apc*^{Min} *Gas6*$^{-/-}$ mice was higher than that in *Apc*^{Min} *Gas6*$^{+/+}$ mice, resulting in shorter survival. In a group of 62 patients with advanced colorectal cancer, Gas6 immunoreactivity in cancer tissues was positively correlated with prognosis. Thus, we revealed a unique *in vivo* inhibitory role of Gas6 during the progression of intestinal tumors associated with suppression of stromal immune reactions. These results suggest a novel therapeutic approach for colorectal cancer patients by regulation of stromal immune responses.

Introduction

Colorectal cancer is one of the most common cancers in the world. To discover novel therapeutic strategies, the mechanisms of colorectal cancer development should be understood. In contrast to other cancers, colorectal cancer develops in a unique organ that harbors a vast population of microbes [1]. Accumulating evidence has indicated a crucial role of Toll-like receptor (TLR) signaling in the interaction between luminal microbes and intestinal tumorigenesis [2-4].

TAM tyrosine kinase receptors (Tyro3, Axl, and Mer) exert pleiotropic effects [5]. Recent studies have shown that TAM receptors inhibit TLR-mediated inflammatory responses in dendritic cells and macrophages [5, 6]. *Tyro3*$^{-/-}$*Axl*$^{-/-}$*Mer*$^{-/-}$ triple knockout mice exhibit a broad spectrum of autoimmune diseases [7]. TAM receptors share two humoral ligands: protein S and growth arrest-specific gene 6 (Gas6) [8, 9]. Protein S is a well-defined vitamin-K-dependent plasma glycoprotein that serves as a cofactor of protein C in the inactivation of Factor Va and VIIIa in the anti-coagulation pathway. Gas6 is a γ-carboxyglutamic acid (Gla) domain-containing protein that was originally described in growth-arrested fibroblasts [10, 11]. Gas6 has the same domain organization as, and 43% amino acid identity with, protein S, and has the potential to induce platelet-mediated thrombosis. Both protein S and Gas6 effectively inhibit TLR-induced cytokine production in mouse dendritic cells and macrophages [5, 6, 12, 13]. For example, TAM activation by Gas6 inhibits production of inflammatory cytokines, such as TNF-α, induced by TLR3, 4, and 9 [6]. Taken together with the recent findings regarding the role of innate immunity in intestinal tumorigenesis [2-4], it

may be beneficial to investigate the potential involvement of TAM receptors and their ligands in intestinal tumor progression.

Among TAM receptors and two ligands, Axl and Gas6 have been particularly focused on in the field of tumor biology. Axl is associated with clinical outcome of leukemia, melanoma, and lung, prostate, ovarian, renal, thyroid, and gastric cancers [14-18]. Axl has transforming effects on human cancer cell lines [19, 20]. In contrast, although several reports have demonstrated the role of Gas6 in tumorigenesis by using cancer cell lines [15, 16, 21], the *in vivo* role of Gas6 in mouse tumor development or human colorectal cancer progression remains to be elucidated.

In this study, we sought to investigate the role of Gas6 during tumorigenesis in *in vivo* intestines using *Gas6*$^{+/+}$ and *Gas6*$^{-/-}$ mice.

Materials & Methods

Cell culture and reagents

Human colorectal cancer cell lines (SW480 and HT29) and a human macrophage cell line (THP-1) were obtained from the American Type Culture Collection (Manassas, VA, USA). Cell lines were cultured in RPMI-1640 (Invitrogen, Carlsbad, CA, USA), supplemented with 10% fetal calf serum (FCS). Recombinant human Gas6, a γ-glutamyl carboxylated active form, was purchased from R&D Systems (Minneapolis, MN, USA).

Cell proliferation assay

SW480 and HT29 cells were seeded at a density of 2.5×10^3 per well in 96-well tissue culture plates; after 24 hours, the medium was changed to FCS-free medium. After 24-hour incubation under the indicated conditions, cell proliferations were measured using the MTS assay (Cell Counting Kit 8; Dojindo, Kumamoto, Japan) according to the manufacturer's protocol.

Animal model of colitis and intestinal tumorigenesis

Generation of Gas6 knockout mouse with a C57/BL6 background was described previously [22]. *Apc*^{Min} mice were obtained from the Jackson Laboratory (Bar Harbor, ME, USA). Animals were housed under specific pathogen-free conditions at the Animal Facilities of Kyoto University. All animal experiments were performed in accordance

with institutional guidelines, and the Review Board of Kyoto University granted an ethical permission for this study. Isolations of mouse epithelial cells and stromal monocytes were described previously [23]. To analyze colitis-associated tumorigenesis, mice were injected with a single intraperitoneal dose of azoxymethane (AOM) (12 mg/kg body weight; Sigma, St. Louis, MO, USA) at the age of 8 weeks and received 2.0% dextran sulfate sodium (DSS) for 5 days 3 times every 3 weeks (Supplementary Figure 1A). To analyze the severity of colitis, mice were sacrificed after the administration of 2.5% DSS for 7 days (Supplementary Figure 1B).

Real-time quantitative reverse- transcription polymerase chain reaction (qRT-PCR)

Total RNA was extracted using Trizol (Invitrogen). Single-strand complementary DNA (cDNA) was synthesized using Transcriptor First Strand cDNA Synthesis Kit (Roche Applied Science, Basel, Switzerland). qRT-PCR was performed using SYBR Green I Master (Roche Applied Science) and Light Cycler 480 (Roche Applied Science). Values are expressed as arbitrary units relative to glyceraldehyde 3-phosphate dehydrogenase (GAPDH). Primer sets used are summarized in Supplementary Table 1.

Generation of bone marrow chimeric mice

Cell suspensions from male *Gas6*$^{+/+}$ and *Gas6*$^{-/-}$ mouse bone marrow were prepared from femurs and tibias, filtered, and counted. Female or male mice received a single intravenous injection of 1×10^7 bone marrow cells, after being lethally irradiated with 10 Gy X-rays. The following groups of chimeric mice were generated: *Gas6*$^{+/+}$ to

Gas6$^{+/+}$, *Gas6*$^{+/+}$ to *Gas6*$^{-/-}$, *Gas6*$^{-/-}$ to *Gas6*$^{+/+}$, *Gas6*$^{-/-}$ to *Gas6*$^{-/-}$ mice. Genomic DNA was extracted from blood 4 weeks later, and bone marrow chimerism was determined by PCR for the *Gas6* and Y chromosome–linked *Sry* genes.

Histological and immunohistochemical analyses

Mouse intestinal tissues were routinely processed. Anti-Tyro3, Axl, Mer, ß-actin, and phosphorylated p65 (Cell Signaling Technology, Danvers, MA, USA), anti-Gr1 (eBioscience, San Diego, CA, USA), anti-F4/80, Socs3, CD45, and TNF-α (Abcam, Cambridge, MA, USA), and anti-Gas6 (Santa Cruz Biotechnology, Santa Cruz, CA, USA) antibodies were used. The primary antibodies were incubated at 4°C overnight, and then secondary antibodies were added. All immunohistochemical analyses were performed with Ig isotype controls or blocking peptides for antibodies.

Enzyme-linked immunosorbent assay

Nuclear protein was extracted from mouse intestinal tissues by using Nuclear Extract Kit (Active Motif, Carlsbad, CA, USA). Protein concentration was measured using Bio-Rad protein assay (Bio-Rad Laboratories, Hercules, CA, USA). DNA binding activity of p65 protein was quantified using TransAM NFκB p65 Transcriptional ELISA Kit (Active Motif).

Clinical sample analysis

Surgically resected specimens were obtained from Stage III/IV colorectal cancer

patients who had been admitted to Kyoto University Hospital. Written informed consent was obtained from all patients with the protocol approved by the Ethics Committee of Kyoto University. Patient's data were anonymously analyzed, and neither the patient nor anyone else could identify the patient with certainty. Sixty-two surgically resected specimens were routinely processed and immunostained. Clinicopathological parameters of those patients are summarized in Supplementary Table 2. Gas6 staining in human cancer specimens was determined to be 'high' when ≥ 50% of the tumor cells were stained with anti-Gas6 antibody and to be 'low' when < 50% of the tumor cells were stained with anti-Gas6 antibody. The number of infiltrating CD45-positive leukocytes was counted in randomly selected 3 high power fields (× 400) in each specimen, and the mean number was determined.

Statistical analysis

Results are presented as the mean values ± standard deviations unless otherwise stated. Difference between treatment, group, and strains were analyzed using the two-tailed Student's *t* test, chi-square test, Fisher's exact test, ANOVA, and Bonferroni's test. Survival rates were estimated by the Kaplan-Meier method and compared using the Gehan-Breslow-Wilcoxon test.

Results

Gas6 enhanced the proliferation of colorectal cancer cells and suppressed the activation of macrophages in vitro

Previous reports using cancer cell lines have suggested that Gas6 contributes to tumor progression [15, 16, 21]. First, we examined the effects of Gas6 on epithelial cells and macrophages *in vitro*. The human colorectal cancer epithelial cell lines, SW480 and HT29 cells, were cultured for 24 hours in serum-free medium containing vitamin K (0.5 μM) with or without recombinant human Gas6 protein (0.5 or 5.0 nM). Both cell lines expressed TAM receptors (Figure 1A), and MTS assays showed that the addition of Gas6 protein weakly, but significantly, enhanced the proliferation of both cell lines (Figure 1B). In addition, mRNA expression of inflammatory cytokines, such as TNF-α and IL-8, were not altered after stimulation with LPS in SW480 and HT29 cells (100 ng/ml; data not shown). Administration of LPS to THP-1 cells, a human macrophage cell line strongly expressing TAM receptors (Figure 1A), pretreated with 100 nM phorbol-12-myristate-13-acetate (PMA) induced the mRNA expression of inflammatory cytokines such as TNF-α and IL-8 2 hours after LPS stimulation (Figure 1C). However, the simultaneous administration of 0.5 nM human Gas6 significantly reduced LPS-induced mRNA expression of TNF-α and IL-8. In addition, the mRNA expression of SOCS1/3 was significantly enhanced in PMA/LPS-stimulated THP-1 cells after incubation with 0.5 nM recombinant Gas6 for 2 hours (Figure 1D). Concomitantly, immunocytochemistry showed that the nuclear accumulation of phosphorylated-p65 in

PMA/LPS-stimulated THP-1 cells was significantly reduced at 2 hours after incubation with 0.5 nM recombinant Gas6 (Figure 1E and F). Thus, Gas6 has an *in vitro* potential to promote the proliferation of colon cancer cells and to suppress the activation of immune responses in macrophages.

Gas6 deficiency enhanced mouse colitis-associated tumorigenesis

Next, we investigated whether Gas6 affects mouse colitis-associated tumorigenesis. Under physiological conditions, the status of epithelial cells, stromal infiltration by inflammatory cells, and mRNA expression of TAM receptors were not altered in relation to the *Gas6* gene dosage (data not shown). However, after azoxymethane/dextran sulfate sodium (AOM/DSS) treatment (Supplementary Figure 1A), the number of polyps in the $Gas6^{-/-}$ mouse colon was significantly greater than that in the $Gas6^{+/+}$ mouse colon (Figure 2A and B). Consistent with this, mRNA expression of proliferation cell nuclear antigen (PCNA) in the colonic polyps of the $Gas6^{-/-}$ mice was significantly higher than that in the polyps of the $Gas6^{+/+}$ mice (Figure 2C). Infiltration of neutrophils and macrophages into colonic polyps of the $Gas6^{-/-}$ mice was more prominent (Figure 2D). In addition, mRNA expression of inflammatory cytokines, such as TNF-α, CXCL1, and CCL2 was significantly upregulated in the colonic polyps of the $Gas6^{-/-}$ mice (Figure 2E). NFκB was also significantly activated (phosphorylation of p65) in the colonic polyps of the $Gas6^{-/-}$ mice (Figure 2F). The mRNA expression of representative tumor-promoting factors, such as c-Myc and Cox2 (Ptgs2), was significantly upregulated in the colonic polyps of the $Gas6^{-/-}$ mice (Figure

2G). After AOM/DSS treatment, survival of the *Gas6*$^{-/-}$ mice was significantly shorter than that of the *Gas6*$^{+/+}$ mice ($P < 0.01$; Figure 2H). Thus, contrary to *in vitro* studies, Gas6 played an inhibitory role in colitis-associated tumorigenesis in mice.

Gas6 was increased locally and appeared to suppress immune responses of infiltrating stromal cells in DSS-induced mouse colitis

Persistent colitis is a risk factor for the progression of colonic tumors [24, 25]. Therefore, it would be possible in the AOM/DSS-treated *Gas6*$^{-/-}$ mice that inflammatory responses in the stromal cells (*e.g.,* macrophages) played a pivotal role in enhancing polyp formation. To confirm whether Gas6 inhibits mouse colitis *in vivo*, we administered DSS to the *Gas6*$^{+/+}$ and *Gas6*$^{-/-}$ mice (Supplementary Figure 1B).

After administration of 2.5 % DSS for 7 days, the *Gas6*$^{-/-}$ mice exhibited more severe colitis than the *Gas6*$^{+/+}$ mice. In the *Gas6*$^{-/-}$ mice, the colonic crypt architecture was almost completely obliterated, with massive stromal infiltration by inflammatory cells, whereas in the *Gas6*$^{+/+}$ mice the crypt architecture was relatively preserved (Figure 3A). The histological damage score [26] and weight loss of the DSS-treated *Gas6*$^{-/-}$ mice were significantly greater than those of the DSS-treated *Gas6*$^{+/+}$ mice (Figure 3B). Stromal infiltration by neutrophils and macrophages was more prominent in the DSS-treated *Gas6*$^{-/-}$ mice (Figure 3C). Similarly, mRNA expression of TNF-α, CXCL1, and CCL2 was significantly higher in the DSS-treated *Gas6*$^{-/-}$ mice (Figure 3D). Thus, Gas6 had inhibitory activity in mouse colonic inflammation in the DSS-treated mice as well as in AOM/DSS-treated mice.

In the DSS-treated *Gas6*$^{+/+}$ mouse colon, Gas6 mRNA expression was significantly increased (Figure 4A), suggesting that locally produced Gas6 plays a role in DSS-induced colitis. Therefore, we sought to evaluate the *in vivo* activation of targets of Gas6/TAM. The mRNA expression of Socs1/3, which are key mediators of Gas6/TAM signaling in the downregulation of TLR-mediated immune responses of macrophages [6], was significantly lower in the DSS-treated *Gas6*$^{-/-}$ mouse colon than in the DSS-treated *Gas6*$^{+/+}$ mouse colon (Figure 4A). ELISA showed that the phosphorylation level of nuclear p65, which is the downstream of TLRs and can be downregulated by Gas6/TAM signaling in macrophages [6], increased significantly in the DSS-treated *Gas6*$^{-/-}$ mice (Figure 4B). Thus, we confirmed that the activation of TLR/Gas6/TAM signaling in DSS-induced colitis was altered according to the Gas6 genotype.

We next performed immunostainings to determine the cell types in which these downstream molecules of Gas6/TAM signaling were activated. Stainings for Socs3 and phosphorylated-p65 were only partially observed in the non-inflamed *Gas6*$^{+/+}$ and *Gas6*$^{-/-}$ mouse colons (Figure 4C, ascending, arrowheads). In contrast, Socs3 and phosphorylated-p65 were vigorously observed in mononuclear cells infiltrating the stroma especially in the inflamed part of the *Gas6*$^{-/-}$ mouse colon (Figure 4C, rectum). Because mRNA expression of TAM receptors in stromal monocytes were slightly higher than those in epithelial cells (data not shown), these results suggest that locally increased levels of Gas6 suppresses innate immune responses in DSS-induced colitis by upregulation of Socs1/3 and downregulation of NFκB in infiltrating stromal cells.

Gas6 from both epithelial cells and bone marrow (BM)-derived cells contributed to suppression of DSS-induced mouse colitis

Previous reports have demonstrated that Gas6 is secreted by various cell types, such as tumor cells, fibroblasts, neutrophils, and macrophages [10, 21, 27]. Consistent with this, there was no significant difference in Gas6 mRNA expression between isolated intestinal epithelial cells and stromal monocytes, and immunostaining against Gas6 was ubiquitous in both residual epithelial cells and stromal inflammatory cells in the DSS-treated *Gas6*$^{+/+}$ mice (data not shown). These data suggest that both epithelial and infiltrating stromal cells produce Gas6. To determine the cellular sources of Gas6 that suppressed DSS-induced colitis, we performed BM transplantations using *Gas6*$^{+/+}$ and *Gas6*$^{-/-}$ mice. Under physiological conditions, there was no evident difference in any mice undergoing BM transplantation (data not shown). After administration of 2.5% DSS for 7 days, the *Gas6*$^{-/-}$ mice transplanted with *Gas6*$^{-/-}$ marrow exhibited the most severe colitis, based on histological damage scores and weight loss (Supplementary Figure 3A-C). The *Gas6*$^{+/+}$ mice transplanted with *Gas6*$^{+/+}$ marrow showed the least severe colitis. *Gas6*$^{-/-}$ mice transplanted with *Gas6*$^{+/+}$ marrow and *Gas6*$^{+/+}$ mice transplanted with *Gas6*$^{-/-}$ marrow exhibited nearly the same degree of moderately severe colitis. Furthermore, the mRNA expression of inflammatory cytokines, such as TNF-α and CXCL1, was altered in parallel with the histological changes (Supplementary Figure 3D). Thus, Gas6 from both epithelial cells and BM-derived cells may contribute to suppression of DSS-induced mouse colitis.

Gas6 deficiency enhanced intestinal tumorigenesis in the Apc^{Min} mice

Most human colorectal cancers develop in a 'multistep' manner without obvious inflammation. Using Apc^{Min} mice, we examined the role of Gas6 in multistep intestinal tumorigenesis. Nontumorous intestinal mucosa in the Apc^{Min} $Gas6^{-/-}$ mice does not show histologically detectable inflammation as well as that in the simple $Gas6^{-/-}$ mice (data not shown). The number of polyps in the small intestine and colon of the Apc^{Min} $Gas6^{-/-}$ mice was significantly greater than that in the Apc^{Min} $Gas6^{+/+}$ mice (Figure 5A and B, and Supplementary Figure 4). PCNA mRNA expression was significantly elevated in the intestinal polyps of the Apc^{Min} $Gas6^{-/-}$ mice compared with that in the intestinal polyps of the Apc^{Min} $Gas6^{+/+}$ mice (Figure 5C). Production of inflammatory cytokines, such as TNF-α, CXCL1, and CCL2 was significantly increased in the intestinal polyps of Apc^{Min} $Gas6^{-/-}$ mice (Figure 5C). NFκB was significantly activated in the intestinal polyps of the Apc^{Min} $Gas6^{-/-}$ mice (Figure 5D). The mRNA expression of c-Myc and Cox2 (Ptgs2), a downstream target of NFκB, was also significantly upregulated in the intestinal polyps of the Apc^{Min} $Gas6^{-/-}$ mice (Figure 5C). Consistently, the Apc^{Min} $Gas6^{-/-}$ mice showed more severe anemia (Figure 5E) with significantly shorter survival compared with the Apc^{Min} $Gas6^{+/+}$ mice ($P < 0.001$; Figure 5F). Thus, Gas6 suppresses multistep tumorigenesis as well as colitis-associated tumorigenesis in mouse intestines.

Elevated Gas6 was associated with better prognosis in advanced colorectal cancer patients

To determine the role of Gas6 in human colorectal cancer, we immunostained surgically resected specimens of 62 colorectal cancer patients (Figure 6A), and compared patient survival. Higher expression of Gas6 in cancer tissues was associated with better survival in stages III (Figure 6B, left) and IV (Figure 6B, right, $P < 0.05$), and overall advanced colorectal cancer patients (Figure 6C, $P < 0.05$). Similar to murine models, increased expression of Gas6 was also significantly associated with decreased infiltration by CD45-positive leukocytes and lower expression of TNF-α (Supplementary Table 3). These results suggest that Gas6 plays an inhibitory role in human colorectal cancer progression and suppression of local inflammatory responses.

Discussion

Previous studies have suggested that Gas6 promotes cancer cell progression *in vitro* [15, 16]. A previous study demonstrated that Gas6 produced from BM-derived cells enhances proliferation of subcutaneously transplanted murine colon cancer cells lacking Gas6 [21]. In this study, we also observed that Gas6 weakly, but significantly, enhances proliferation of human cancer cell lines. Importantly, these effects of Gas6 are exerted at cellular levels. The role of Gas6 should be complicated during *in vivo* intestinal tumorigenesis, because the intestines are inhabited by a vast population of microbes that play important roles in intestinal tumorigenesis [1-4]. In line with previous studies [5, 6, 12, 13], we also showed that Gas6 suppressed innate immune responses of a human monocyte cell line.

We analyzed AOM/DSS intestinal tumor formation model, and revealed that the number of polyps in the *Gas6*$^{-/-}$ mice was greater than that in the *Gas6*$^{+/+}$ mice. Persistent colitis is a well-known risk factor for the progression of colonic tumors both in humans and mice [24, 25]. In our study, because the DSS-treated *Gas6*$^{-/-}$ mice exhibited more severe colitis than the DSS-treated *Gas6*$^{+/+}$ mice, it can be reasoned that the absence of *Gas6* and its anti-inflammatory activity was responsible for the increased number of polyps in the AOM/DSS-treated *Gas6*$^{-/-}$ mice. Thus, in contrast to its *in vitro* behavior, the property of Gas6 to inhibit inflammatory cytokine production [5, 6, 12, 13], appears to exert an important negative effect on mouse intestinal tumorigenesis.

In monocyte lineages, Gas6/TAM signaling suppresses NFκB activation and

inflammation through the induction of Socs1/3 [5, 6]. Our BM transplantation experiments showed that Gas6 from both epithelial cells and BM-derived cells contributed to the suppression of DSS-induced mouse colitis. This is in line with the fact that Gas6 is a secretory protein, and the degree of suppression of colitis appeared to be determined by local Gas6 dosage. Because BM transplantation could not directly indicate the target cells of Gas6, we speculated that cells in which NFκB and Soxs1/3 are activated could be the target of Gas6/TAM signaling. In our *in vivo* study, intense immunostaining of phosphorylated p65 and Socs3 was observed in the stromal infiltrating cells rather than the epithelial cells in the DSS-treated inflamed mouse colon. Phosphorylation of p65 and mRNA expression of Socs1/3 were significantly lower in the absence of Gas6. Although not directly, these *in vivo* results suggest that the predominant target of Gas6 was stromal infiltrating cells rather than epithelial cells, and that Gas6 inhibits intestinal inflammation in DSS-induced colitis by suppressing immune responses of stromal monocyte lineages (*e.g.,* macrophages). These results also support the notion that the weak growth-promoting effect of Gas6 on epithelial cells may be overcome by strong immune suppressive effect of Gas6 on monocyte lineages during *in vivo* intestinal tumorigenesis.

It should be noted that similar to the AOM/DSS colitis mice, in the Apc^{Min} mouse model in our study, the number of polyps in the $Gas6^{-/-}$ mice was greater than that in the $Gas6^{+/+}$ mice, thereby resulting in significantly severe anemia and shorter survival. In contrast to the AOM/DSS colitis mouse, the Apc^{Min} mouse is not characterized by the presence of obvious intestinal inflammation. However, polyps from both AOM/DSS and

Apc^{Min} mice are exposed to LPS-producing luminal bacteria. Lack of TLR signaling or microbes suppresses *Apc*^{Min} mouse intestinal tumorigenesis [3, 4]. Furthermore, lack of TNF-α, a key inflammatory cytokine that induces NFκB activation, significantly reduces intestinal polyp formation in *Apc*^{Min} mice [25]. In our study, the activity of NFκB, a downstream target of TLR signaling, and TNF-α mRNA levels were significantly higher in the *Gas6*$^{-/-}$ mice than in the *Gas6*$^{+/+}$ mice with either AOM/DSS treatment or *Apc*^{Min} genotype. Consistent with these data, Cox2 (Ptgs2), a key tumor-promoting factor regulated by NFκB, was also significantly elevated in the *Gas6*$^{-/-}$ mice. Therefore, activation of the TLR/TNF-α-NFκB-Cox2 pathways appears to be one of the important events that promote intestinal tumorigenesis in the absence of *Gas6* in both AOM/DSS-treated and *Apc*^{Min} mouse models.

In humans, we found that higher expression of Gas6 in the cancer tissues was associated with longer survival and a milder local inflammatory responses in colorectal cancer patients. These data are consistent with our murine models and with a previous study showing that high Gas6 expression was associated with better prognosis of renal cancer patients [18]. However, a recent report showed that the activation of AXL is associated with the resistance to EGFR-targeted therapy in lung cancer [16]. In addition, it is important to note that warfarin, which has an inhibitory effect on Gas6 activity by blocking vitamin K-dependent γ-glutamyl carboxylation, is widely used as an anticoagulant. As for the association between warfarin use and the prognosis of cancer patients, a recent large cohort study showed that the effect of warfarin on patient survival was identical to that of placebo in gastrointestinal cancers [28]. Thus, the role

of Gas6 and related factors appears complex, and further studies are required to determine the comprehensive role of Gas6 and TAM receptors in colorectal cancer patients.

In conclusion, we demonstrated that Gas6 has an inhibitory effect on intestinal tumorigenesis *in vivo*. Although additional clinical studies are required to clarify the roles of Gas6 in human colorectal cancers, our results may provide clues for developing novel therapeutic strategies against colorectal cancer by regulating stromal immune responses.

Funding

This work was supported by the Japan Society for the Promotion of Science (JSPS) KAKENHI 21229009, 23590937, 24229005, 24590914, 24590916, and 24659363; Research program of the Project for Development of Innovative Research on Cancer Therapeutics (P-Direct) from Ministry of Education, Culture, Sports, Science and Technology of Japan; Health and Labour Sciences Research Grants for Research on Intractable Diseases, Hepatitis, and The innovative development and the practical application of new drugs for hepatitis B from the Ministry of Health, Labour and Welfare, Japan; the Funding Program for Next-Generation World-leading Researchers (LS075), Grants-in Aid from the Ministry of Education, Culture, Science, Sports and Technology of Japan; Princess Takamatsu Cancer Research Fund 10-24212, Japan.

Acknowledgements

We are grateful to Dr. Toru Nakano for kindly providing essential materials. We also thank Dr. Shoko Ishizu for technical assistance.

Conflict of Interest

All authors have no conflict of interests.

References

1. Hooper, L.V. et al. (2001) Commensal host-bacterial relationships in the gut. *Science*, **292**, 1115–1118.

2. Rakoff-Nahoum, S. et al. (2007) Regulation of spontaneous intestinal tumorigenesis through the adaptor protein MyD88. *Science*, **317**, 124-127.

3. Rakoff-Nahoum, S. et al. (2009) Toll-like receptors and cancer. *Nat Rev Cancer*, **9**, 57-63.

4. Fukata, M. et al. (2010) Microflora in colorectal cancer: a friend or fear. *Nat Med*, **16**, 639-641.

5. Lemke, G. et al. (2008) Immunobiology of the TAM receptors. *Nar Rev Immunol*, **8**, 327-336.

6. Rothlin, C.V. et al. (2007) TAM receptors are pleiotropic inhibitors of the innate immune response. *Cell*, **131**, 1124-1136.

7. Lu, Q. et al. (2001) Homeostatic regulation of the immune system by receptor tyrosine kinases of the Tyro3 family. *Science*, **293**, 306-311.

8. Stitt, T.N. et al. (1995) The anticoagulation factor Protein S and its relative, Gas6, are ligands for the Tyro3/Axl family of receptor tyrosine kinases. *Cell*, **80**, 661-670.

9. Varnum, B.C. et al. (1995) Axl receptor tyrosine kinase stimulated by the vitamin K-dependent protein encoded by growth-arrest-specific gene 6. *Nature*, **373**, 623-626.

10. Manfioletti, G. et al. (1993) The protein encoded by a growth arrest-specific gene (gas6) is a new member of the vitamin K-dependent proteins related to protein S, a negative coregulator in the blood coagulation cascade. *Mol Cell Biol*, **13**, 4976-4985.

11. Hafizi, S. et al. (2006) Gas6 and protein S. Vitamin K-dependent ligands for the Axl receptor tyrosine kinase subfamily. *FEBS J*, **273**, 5231-5244.

12. Fernández-Fernández, L. et al. (2008) Growth arrest-specific gene 6 (Gas6). *Thromb Haemost,* **100**, 604-610.

13. Caraux, A. et al. (2006) Natural killer cell differentiation driven by Tyro3 receptor tyrosine kinases. *Nat Immunol*, **7**, 747-754.

14. Dirks, W. et al (1999) Expression of the growth arrest-specific gene 6 (GAS6) in leukemia and lymphoma cell lines. *Leuk Res*, **23**, 643-651.

15. Sainaghi, P.P. et al. (2005) Gas6 induces proliferation in prostate carcinoma cell lines expressing the Axl receptor. *J Cell Physiol*, **204**, 36-44.

16. Zhang, Z. et al. (2012) Activation of the AXL kinase causes resistance to EGFR-targeted therapy in lung cancer. *Nat Genet*, **44**, 852-860.

17. Sawabu, T. et al. (2007) Growth arrest-specific gene 6 and Axl signaling enhances gastric cancer cell survival via Akt pathway. *Mol Carcinog*, **46**, 155-164.

18. Gustafsson, A. et al. (2009) Differential expression of Axl and Gas6 in renal cell carcinoma reflecting tumor advancement and survival. *Clin Cancer Res*, **15**, 4742-4749.

19. Zhang, Q.K. et al. (1996) Transforming activity of retroviral genomes encoding Gag-Axl fusion proteins. *J Virol*, **70**, 8089-8097.

20. Song, X. et al. (2010) Overexpression of receptor tyrosine kinase Axl promotes tumor cell invasion and survival in pancreatic ductal adenocarcinoma. *Cancer*, **117**, 734-743.

21. Loges, S. et al. (2010) Malignant cells fuel tumor growth by educating infiltrating leukocytes to produce the mitogen Gas6. *Blood*, **115**, 2264-2273.

22. Yanagita, M. et al. (2002) Essential role of Gas6 for glomerular injury in nephrotoxic nephritis. *J Clin Invest*, **102**, 239-246.

23. Weigmann, B. et al. (2007) Isolation and subsequent analysis of murine lamina propria mononuclear cells from colonic tissue. *Nat Protoc*, **2**, 2307-2311.

24. Karin, M. et al. (2005) NF-kappaB: linking inflammation and immunity to cancer development and progression. *Nat Rev Immunol*, **5**, 749-759.

25. Rao, V.P. et al. (2006) Proinflammatory CD4+CD45RBhi lymphocytes promote mammary and intestinal carcinogenesis in ApcMin/+ mice. *Cancer Res*, **66**, 57-61.

26. Rath, H.C. et al. (1996) Normal luminal bacteria, especially Bacteroides species, mediate chronic colitis, gastritis, and arthritis in HLA-B27/human beta2 microglobulin transgenic rats. *J Clin Invest*, **98**, 945-953.

27. Nakano, T. et al. (1995) Vascular smooth muscle cell-derived, Gla-containing growth potentiating factor for Ca2+-mobilizing growth factors. *J Biol Chem*, **270**, 5702-5705.

28. Rothwell, P.M. et al. (2011) Effect of daily aspirin on long-term risk of death due to cancer: analysis of individual patient data from randomised trials. *Lancet*, **377**, 31-41.

Figure Legends

Figure 1. Administration of GAS6 enhanced proliferation of colon epithelial cells and suppressed immune reactions of macrophages.

(A) Western blotting showed protein expression of TAM receptors in SW480 and HT29, human colon cancer cell lines, and THP-1, a human macrophage cell line. ß-ACTIN was shown as a control.

(B) SW480 and HT29 cells were incubated in a serum-free medium containing vitamin K (0.5 μM) with or without recombinant human GAS6 protein. After 24-hour incubation, cellular proliferation was measured using the MTS assay (mean ± SD, n = 5 each). *$P < 0.05$.

(C and D) THP-1 cells pretreated with PMA (100 nM) were administered LPS (100 ng/ml) with or without recombinant GAS6 (0.5 nM). After 2 hours, RNA was extracted and mRNA expression was evaluated by qRT-PCR (mean ± SD, n = 5 each). *$P < 0.05$

(E) Representative immunostainings of nuclear accumulated phosphorylated (p)-p65 after 2-hour incubation with and without 0.5 nM recombinant GAS6 in PMA-stimulated (left) and PMA/LPS-stimulated (right) THP-1 cells. Bars, 10μm.

(F) Percentages p-p65-immunostained THP-1 cells were evaluated by immunostainings for p-p65 (mean ± SD, n = 5 each). *$P < 0.05$

Figure 2. Deficiency of Gas6 enhanced mouse AOM/DSS-induced colonic polyp formation.

(A) Representative histology of the colonic polyp in *Gas6*$^{+/+}$ and *Gas6*$^{-/-}$ mice after the administration of AOM/DSS. Dotted lines indicate polyp margins. Bars, 200μm.

(B) Total polyp numbers (left) and those in indicated size fractions (right) in *Gas6*$^{+/+}$ and *Gas6*$^{-/-}$ mice after the administration of AOM/DSS (mean ± SD/mouse, n = 10 each). **P* < 0.05

(C, E, and G) RNA was extracted from colonic polyps, and mRNA expression was evaluated by qRT-PCR in AOM/DSS-treated *Gas6*$^{+/+}$ and *Gas6*$^{-/-}$ mice (mean ± SD, n = 10 mice each). **P* < 0.05

(D) The numbers of Gr-1-positive and F4/80-positive cells in ×400 high power field in AOM/DSS-treated *Gas6*$^{+/+}$ and *Gas6*$^{-/-}$ mouse polyps (mean ± SD, n = 10 each). **P* < 0.05

(F) Nuclear protein was extracted from AOM/DSS-treated *Gas6*$^{+/+}$ and *Gas6*$^{-/-}$ mouse polyps, and phosphorylation of p65 protein was quantified by ELISA (mean ± SD, n = 5 each). **P* < 0.05

(H) There was a significant difference of survival between AOM/DSS-treated *Gas6*$^{+/+}$ and *Gas6*$^{-/-}$ mice (n = 20 each, *P* < 0.01).

Figure 3. Deficiency of Gas6 caused severe DSS-induced mouse colitis.

(A) Representative histology of DSS-treated *Gas6*$^{+/+}$ and *Gas6*$^{-/-}$ moue colon. Note that crypt-like structures (*) were barely preserved in Gas6$^{+/+}$ mouse colon. Bars, 50μm.

(B) Histological damage scores (left) and body weight lossees (right) in DSS-treated *Gas6*$^{+/+}$ and *Gas6*$^{-/-}$ mice (mean ± SD, n = 10 each). Body weight before the

administration of DSS was defined as 100%. *$P < 0.05$

(C) Top; The numbers of Gr-1-positive and F4/80-positive cells in DSS-treated *Gas6*$^{+/+}$ (white bar) and *Gas6*$^{-/-}$ (black bar) mouse colon (mean number/×400 high power field ± SD, n = 10 each). *$P < 0.05$ Bottom; Immunostainings for Gr-1 and F4/80 in DSS-treated *Gas6*$^{+/+}$ and *Gas6*$^{-/-}$ mouse colons. Bars, 50μm.

(D) RNA was extracted from colonic tissues in DSS-treated *Gas6*$^{+/+}$ (white bar) and *Gas6*$^{-/-}$ (black bar) mice, and mRNA expression of each factor was evaluated by qRT-PCR in colonic tissues of DSS-treated *Gas6*$^{+/+}$ and *Gas6*$^{-/-}$ mice (mean ± SD, n = 10 each). *$P < 0.05$

Figure 4. Target molecules of Gas6 were activated in the stroma of DSS-induced mouse colitis.

(A) RNA was extracted from colonic tissues in DSS-treated *Gas6*$^{+/+}$ (white bar) and *Gas6*$^{-/-}$ (black bar) mice, and mRNA expression of each factor was evaluated by qRT-PCR in colonic tissues of DSS-treated *Gas6*$^{+/+}$ and *Gas6*$^{-/-}$ mice (mean ± SD, n = 10 each). *$P < 0.05$

(B) Nuclear protein was extracted from colonic tissues in DSS-treated *Gas6*$^{+/+}$ and *Gas6*$^{-/-}$ mice, and phosphorylation of p65 protein was determined by ELISA (mean ± SD, n = 5 each). *$P < 0.05$

(C) Representative immunostainings against Socs3 and phosphorylated (p)-p65 in DSS-treated *Gas6*$^{+/+}$ and *Gas6*$^{-/-}$ mouse colon. Socs3 and p-p65 immunostainings were observed in epithelial cells in non-inflamed ascending colon (arrowheads). However,

Socs3 and p-p65 were primarily expressed in the stromal infiltrating mononuclear cells in inflamed rectum. Bars, 20μm.

Figure 5. Deficiency of Gas6 promoted intestinal polyp formation in *Apc*^{Min} mice.

(A) Numbers of the intestinal polyps in *Apc*^{Min} *Gas6*$^{+/+}$ and *Apc*^{Min} *Gas6*$^{-/-}$ mice (mean ± SD/mouse, n = 10 each). **P* < 0.05

(B) Numbers of the intestinal polyps in indicated size fractions of *Apc*^{Min} *Gas6*$^{+/+}$ and *Apc*^{Min} *Gas6*$^{-/-}$ mice (mean ± SD/mouse, n = 10 each). **P* < 0.05

(C) RNA was extracted from small intestinal polyps in *Apc*^{Min} *Gas6*$^{+/+}$ and *Apc*^{Min} *Gas6*$^{-/-}$ mice, and mRNA expression was evaluated by qRT-PCR (mean ± SD, n = 10 each). **P* < 0.05

(D) Nuclear protein was extracted from small intestinal polyps in *Apc*^{Min} *Gas6*$^{+/+}$ and *Apc*^{Min} *Gas6*$^{-/-}$ mice, and phosphorylation of p65 protein was quantified by ELISA (mean ± SD, n = 5 each). **P* < 0.05

(E) Hemoglobin concentrations in *Apc*^{Min} *Gas6*$^{+/+}$ and *Apc*^{Min} *Gas6*$^{-/-}$ mice were depicted at the indicated time points (mean ± SD/mouse, n = 5 each, **P* < 0.05).

(F) There was a significant difference of survival between *Apc*^{Min} *Gas6*$^{+/+}$ and *Apc*^{Min} *Gas6*$^{-/-}$ mice (*P* < 0.001).

Figure 6. Elevated Gas6 was associated with better prognosis in advanced colorectal cancer patients.

(A) Representative immunostaining against Gas6 in human colorectal cancer patients.

High expression of Gas6 was observed in cancer cells (Case 1 and 2) and stromal cells (Case 2). Bars, 50μm.

(B) Kaplan-Meier analyses showing that higher expression of Gas6 protein were associated with better survival in stage III (left) and IV (right, $P < 0.05$) colorectal cancer patients.

(C) Kaplan-Meier analysis showing that higher expression of Gas6 protein was significantly associated with better survival in stage III/IV colorectal cancer patients ($P < 0.05$).

Supplementary Figure 1. Schema of drug treatment schedule.

(A) To analyze the colitis-associated intestinal tumorigenesis, AOM (12 mg/kg body weight) was administered intraperitoneally at the beginning of drug treatment. Thereafter, 2.0% DSS was administered *ad libitum* for 5 days 3 times.

(B) To analyze the severity of colitis, 2.5% DSS was administered *ad libitum* for 7 days.

Supplementary Figure 2. Gas6 from both epithelial cells and bone marrow (BM) derived cells contributed to suppress DSS-induced mouse colitis.

(A) Representative histology of DSS-treated each BM-transplanted moue colon. Bars, 50μm.

(B and C) Histological damage scores (B) and body weight losses (C) in DSS-treated BM-transplanted mice (mean ± SD, n = 5 each). Body weight before the administration of DSS was defined as 100% (C). Only *Gas6*$^{-/-}$ mice transplanted with *Gas6*$^{-/-}$ marrow

showed a significant change compared to *Gas6*$^{+/+}$ mice transplanted with *Gas6*$^{+/+}$ marrow. *$P < 0.05$

(D) RNA was extracted from colonic tissues of DSS-treated BM-transplanted mice, and mRNA expression of each cytokine was evaluated by qRT-PCR (mean ± SD, n = 5 each). *$P < 0.05$

Supplementary Figure 3. Intestinal polyp formation in *Apc*^{Min} *Gas6*$^{+/+}$ and *Apc*^{Min} *Gas6*$^{-/-}$ mice.

(A) Representative images of polyps in *Apc*^{Min} *Gas6*$^{+/+}$ and *Apc*^{Min} *Gas6*$^{-/-}$ mouse small intestines. Dotted lines indicate polyp margins. Bars, 100μm.

(B) Representative images of polyps in *Apc*^{Min} *Gas6*$^{+/+}$ and *Apc*^{Min} *Gas6*$^{-/-}$ mouse colons. Dotted lines indicate polyp margins. Bars, 100μm.

Figure 1 Akitake-Kawano et al.

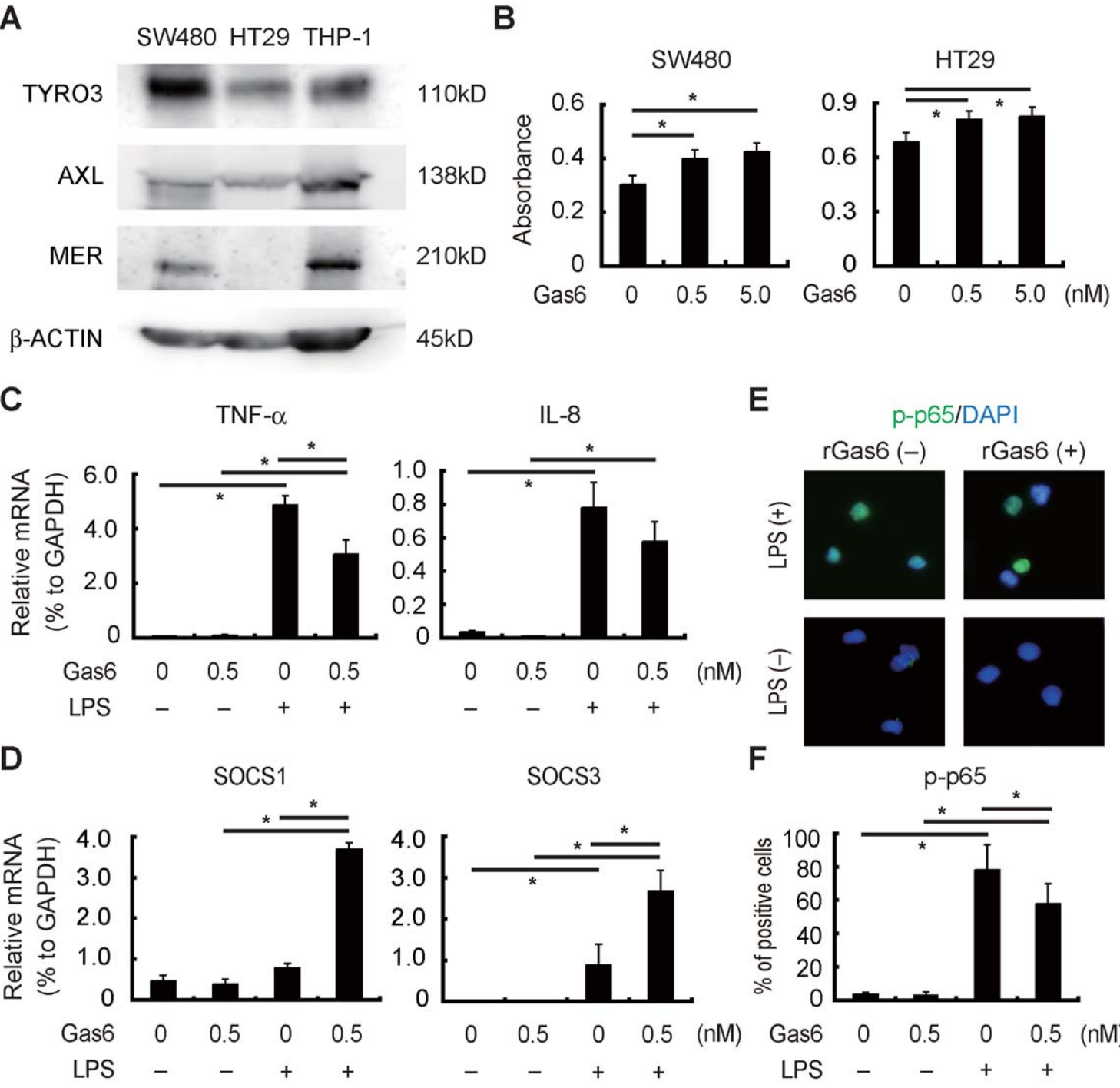

Figure 2 Akitake-Kawano et al.

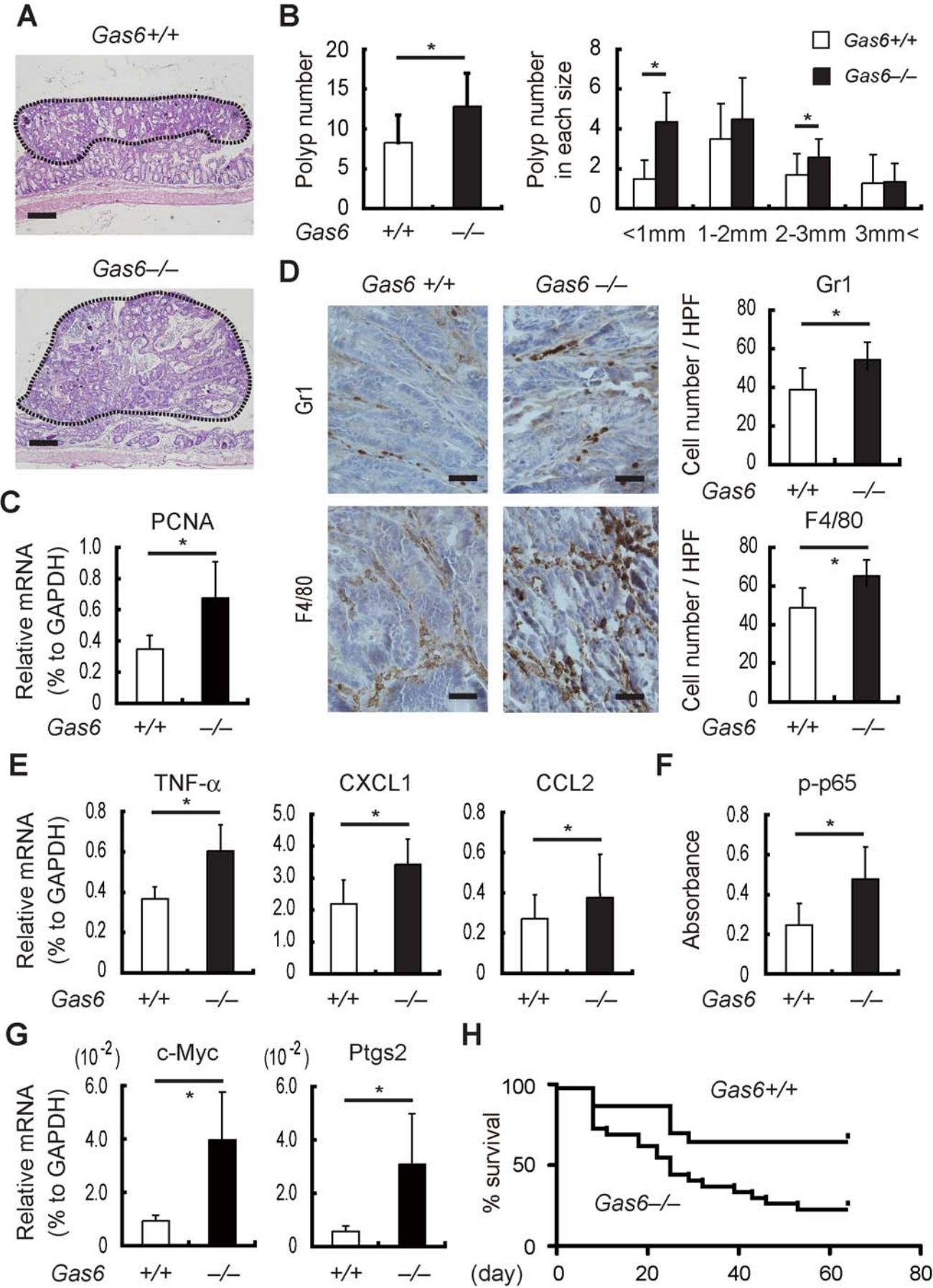

Figure 3 Akitake-Kawano et al.

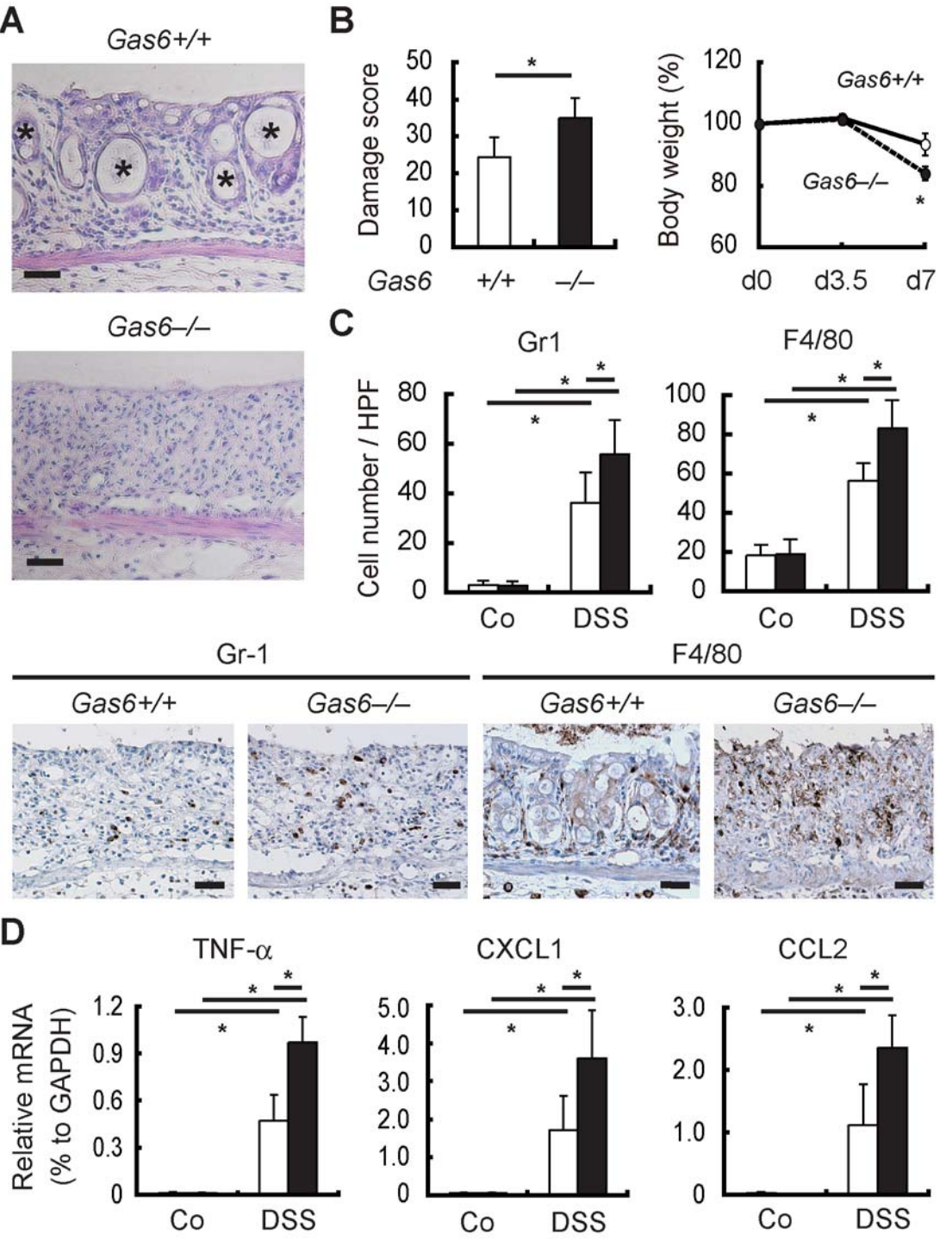

Figure 4 Akitake-Kawano et al.

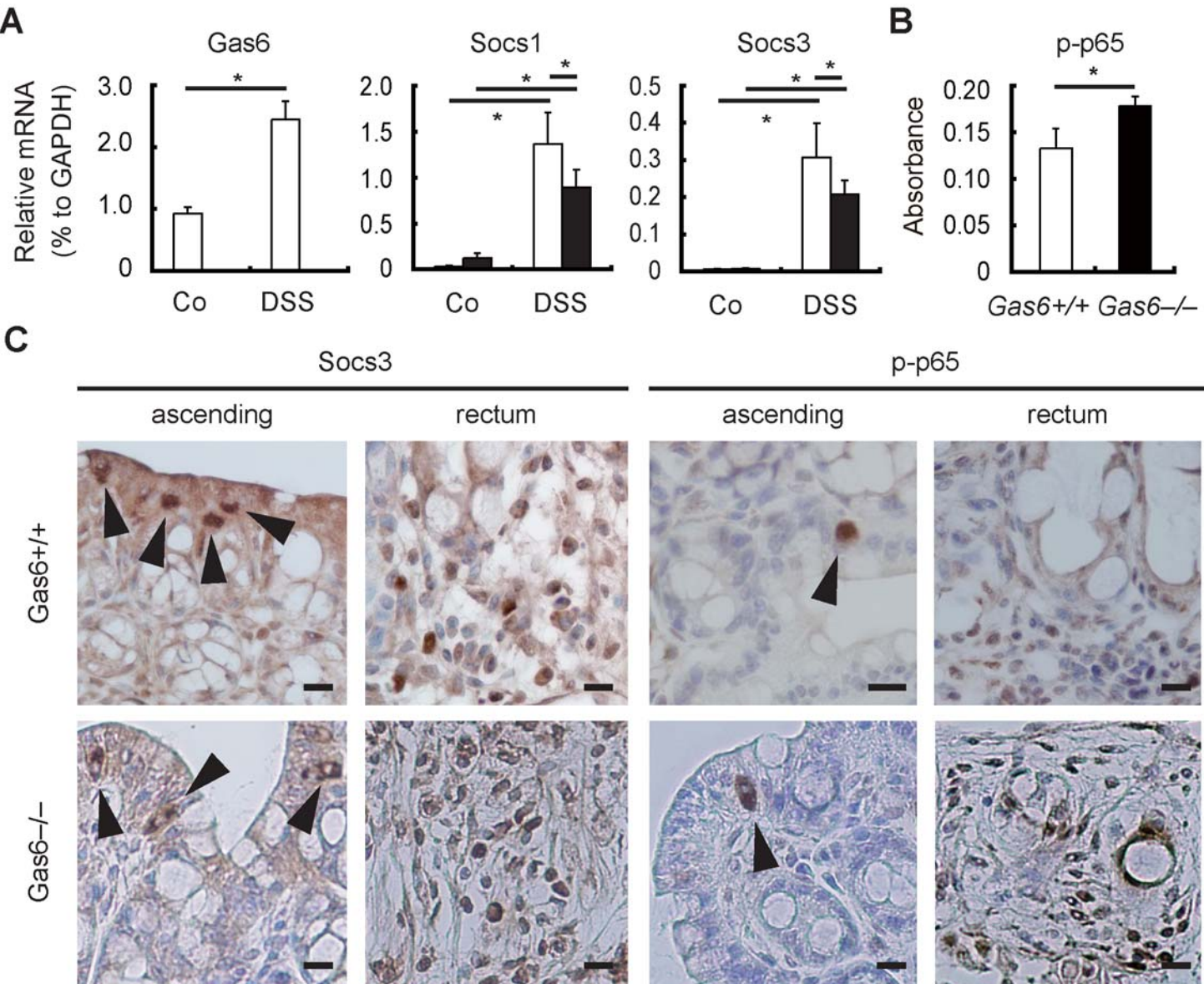

Figure 5 Akitake-Kawano et al.

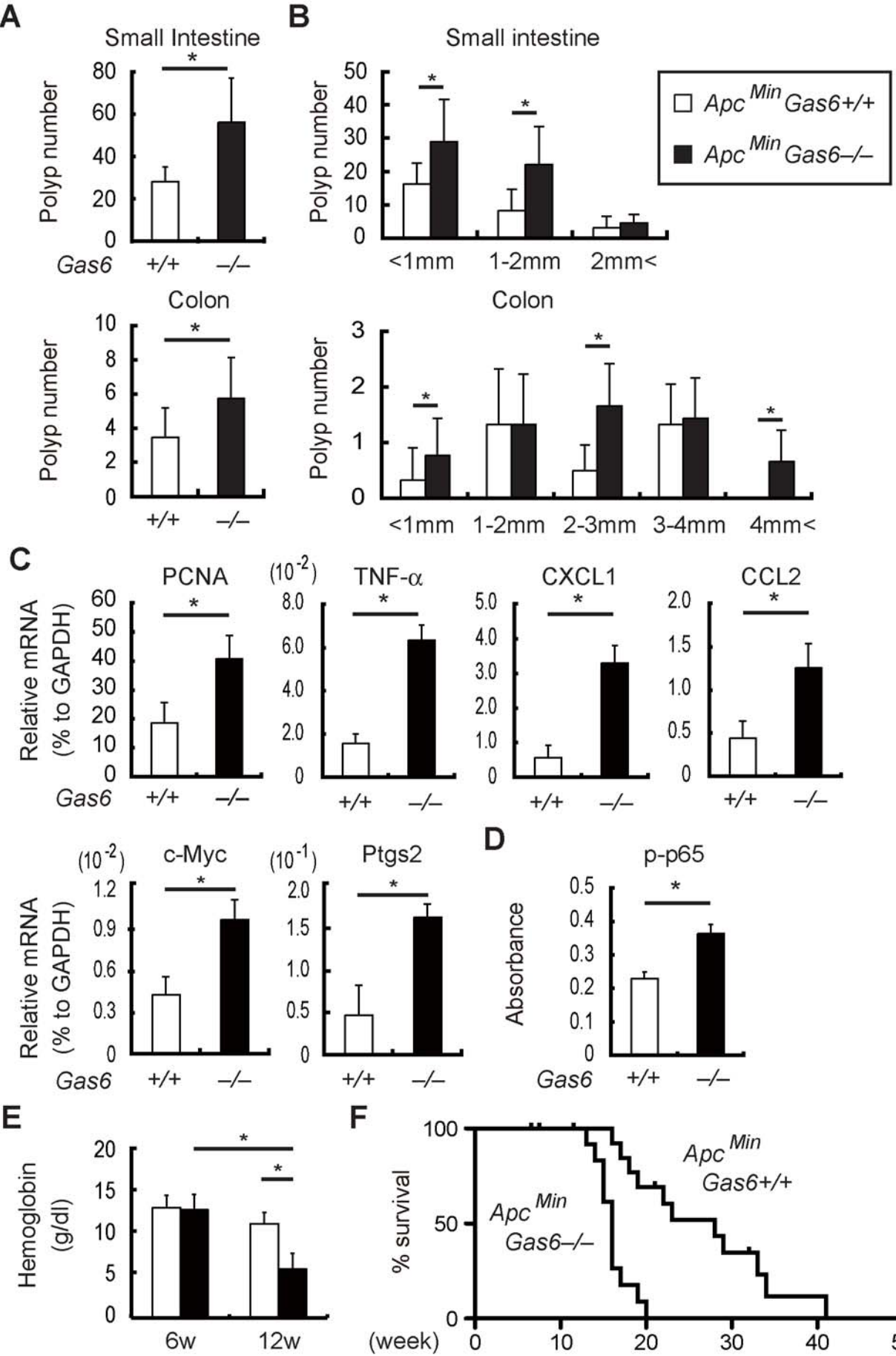

Figure 6 Akitake-Kawano et al.

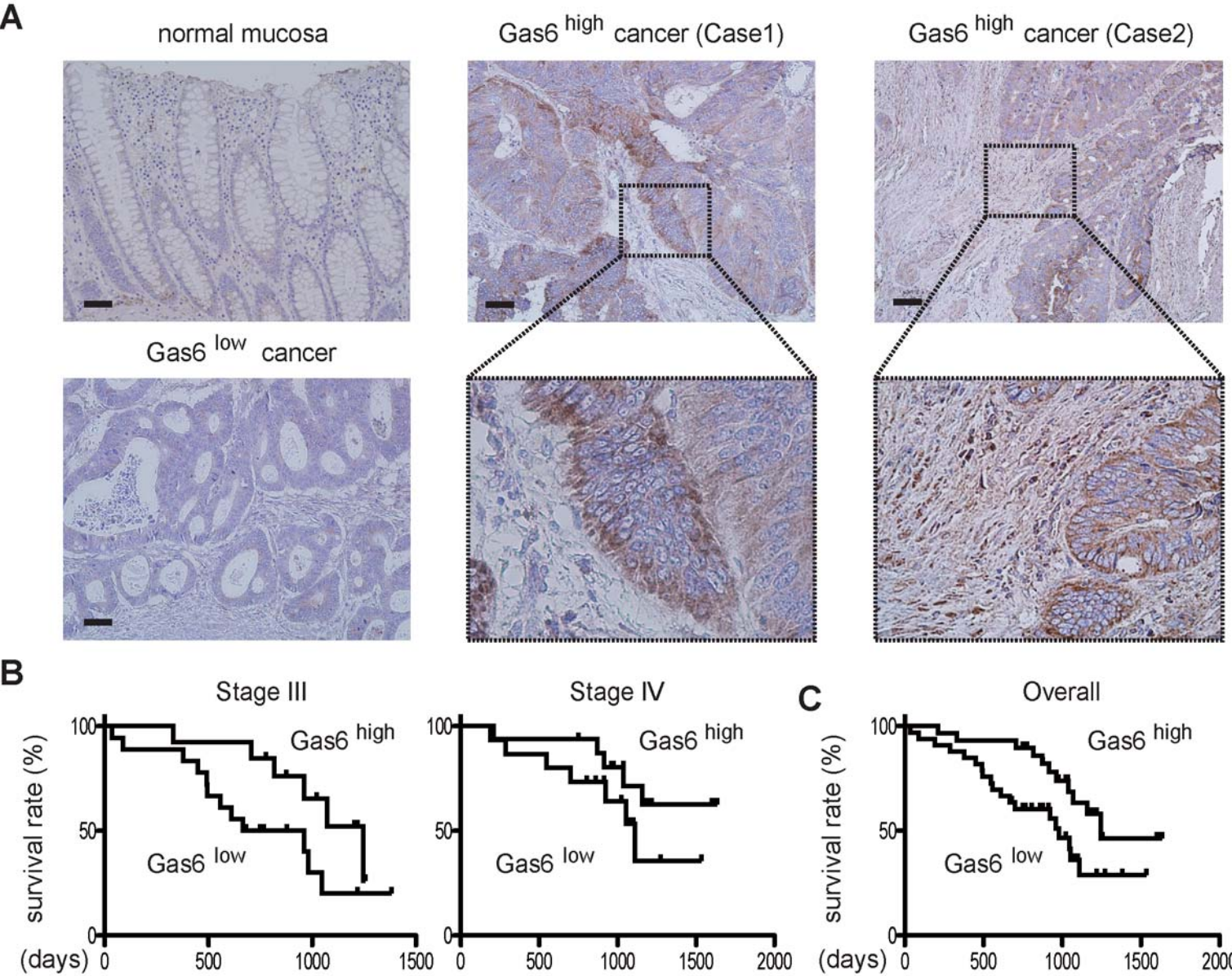

Supplementary Figure 1 Akitake-Kawano et al.

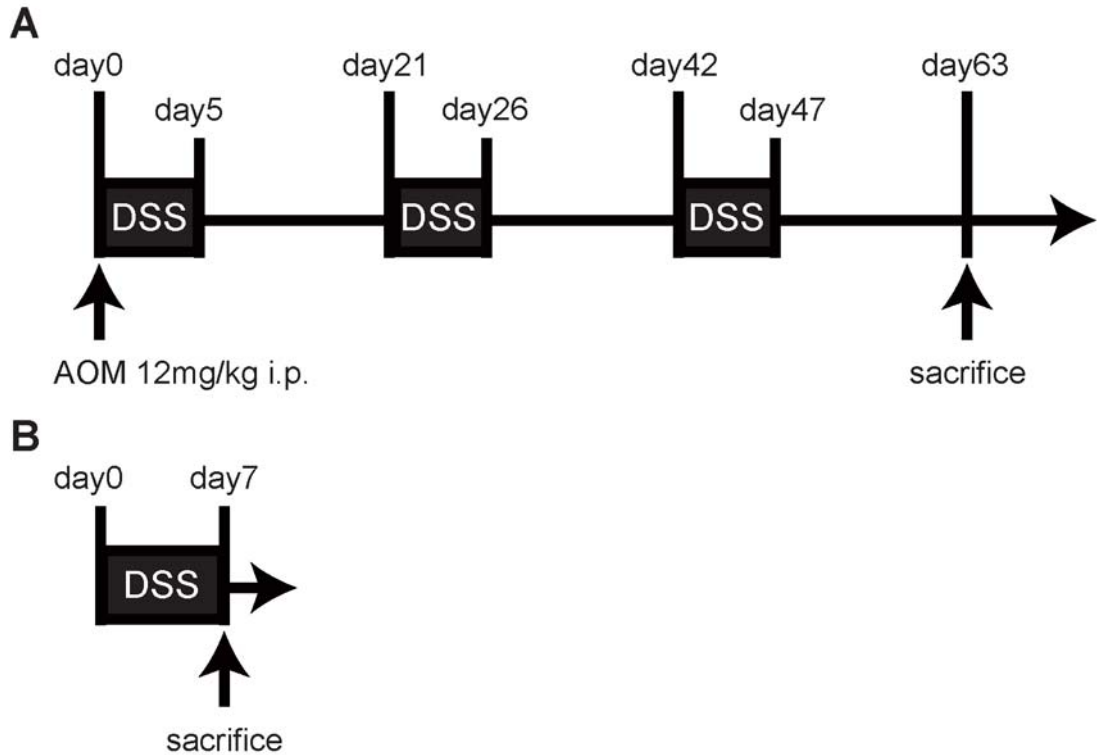

Supplementary Figure 2 Akitake-Kawano et al.

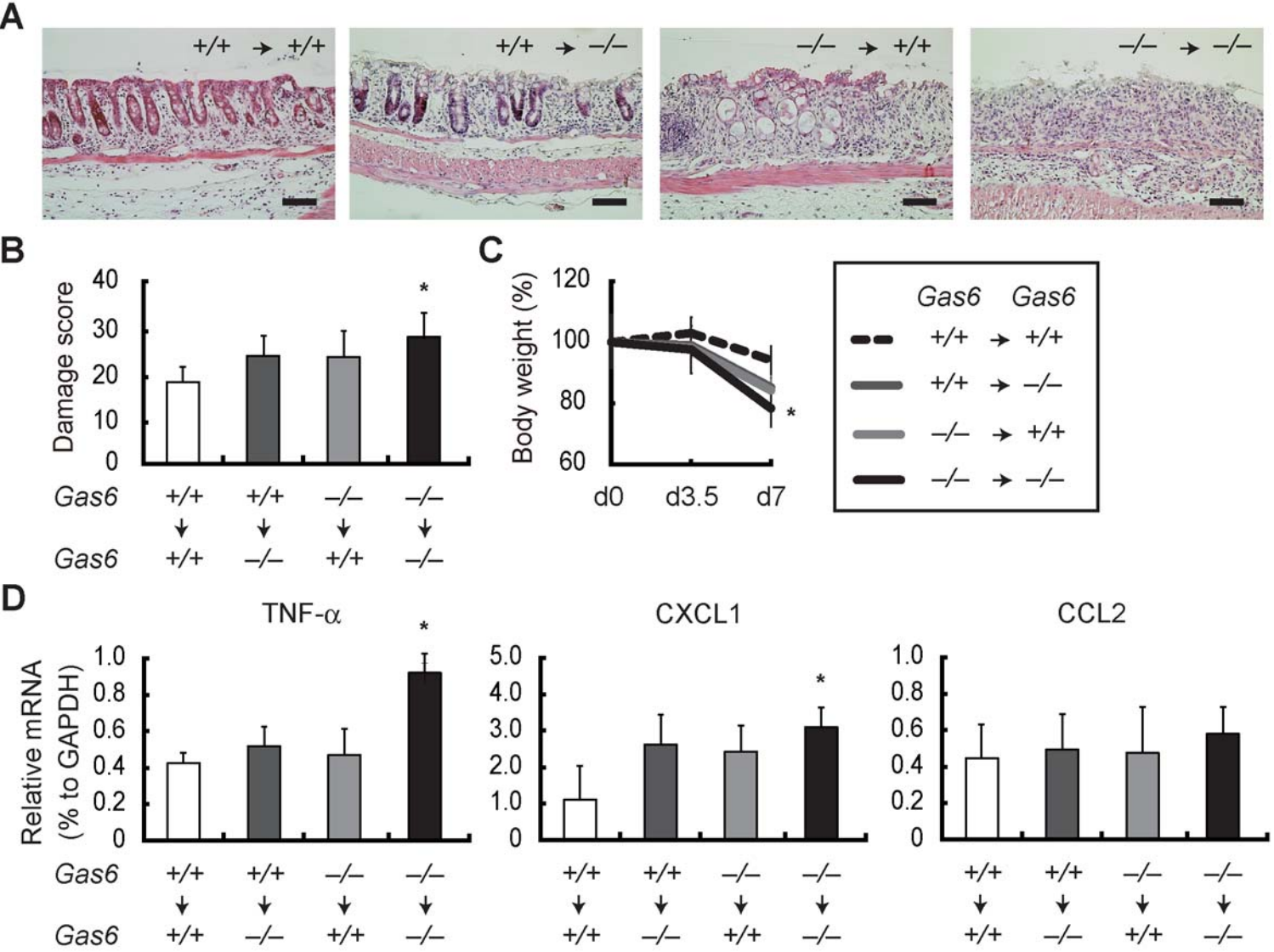

Supplementary Figure 3 Akitake-Kawano et al.